




The superior allele *LEA12^{OR}* in wild rice enhances salt tolerance and yield

Yuwei Ge^{1,†}, Gaoming Chen^{1,†} , Xinran Cheng^{1,†}, Chao Li¹, Yunlu Tian¹, Wenchao Chi¹, Jin Li¹, Zhaoyang Dai¹, Chunyuan Wang¹, Erchao Duan¹, Yan Liu², Zhiguang Sun², Jingfang Li², Baoxiang Wang², Dayong Xu², Xianjun Sun³, Hui Zhang³, Wenhua Zhang⁴, Chunming Wang^{1,5,*}  and Jianmin Wan^{1,3,*} 

¹State Key Laboratory of Crop Genetics & Germplasm Enhancement and Utilization, Nanjing Agricultural University, Nanjing, China

²Lianyungang Academy of Agricultural Science, Lianyungang, Jiangsu, China

³State Key Laboratory of Crop Gene Resources and Breeding, Institute of Crop Sciences, Chinese Academy of Agricultural Sciences, Beijing, China

⁴College of Life Sciences, State Key Laboratory of Crop Genetics & Germplasm Enhancement and Utilization, Nanjing Agricultural University, Nanjing, China

⁵Zhongshan Biological Breeding Laboratory, Southern Japonica Rice R&D Corporation Ltd, Nanjing, China

Received 30 April 2024;

revised 6 June 2024;

accepted 9 June 2024.

*Correspondence (Chunming Wang: Tel + 86-025-84399563; Fax +86-025-84396516; email wangchm@njau.edu.cn; Jianmin Wan: Tel + 86-010-82105837; Fax + 86-010-082105819; email wanjianmin@caas.cn or email wanjm@njau.edu.cn)

[†]These authors contributed equally.

Keywords: rice (*Oryza sativa* L.), wild rice (*Oryza rufipogon* Griff.), superior allele, salt tolerance (ST), late embryogenesis abundant (LEA) protein, abscisic acid (ABA).

Summary

Soil salinity has negative impacts on food security and sustainable agriculture. Ion homeostasis, osmotic adjustment and reactive oxygen species scavenging are the main approaches utilized by rice to resist salt stress. Breeding rice cultivars with high salt tolerance (ST) and yield is a significant challenge due to the lack of elite alleles conferring ST. Here, we report that the elite allele *LEA12^{OR}*, which encodes a late embryogenesis abundant (LEA) protein from the wild rice *Oryza rufipogon* Griff., improves osmotic adjustment and increases yield under salt stress. Mechanistically, *LEA12^{OR}*, as the early regulator of the *LEA12^{OR}-OsSAPK10-OsbZIP86-OsNCED3* functional module, maintains the kinase stability of OsSAPK10 under salt stress, thereby conferring ST by promoting abscisic acid biosynthesis and accumulation in rice. The superior allele *LEA12^{OR}* provides a new avenue for improving ST and yield via the application of *LEA12^{OR}* in current rice through molecular breeding and genome editing.

Introduction

Land salinization threatens global rice (*Oryza sativa* L.) production (Liu *et al.*, 2022; Zhao *et al.*, 2020). Excessive salinity in the soil mainly damages rice by disrupting ion balance (Wang *et al.*, 2020a) and disordering secondary metabolism, as well as by causing water loss through osmotic pressure (Deinlein *et al.*, 2014; Zhao *et al.*, 2020). In response to these challenges, rice has evolved several mechanisms, such as ion homeostasis regulation (Ren *et al.*, 2005; Wang *et al.*, 2020a) and osmotic adjustment (Liu *et al.*, 2022). We recently reported *OsTUB1* and *OsWRKY53* as key regulators stabilizing the ion transporters during ion homeostasis regulation in rice (Chen *et al.*, 2022; Yu *et al.*, 2023). *RST1* encodes an auxin response factor (OsARF18), which is a synergistic regulator of growth and salt tolerance (Deng *et al.*, 2022). To date, while key genes and regulatory mechanisms have been intensively studied for ion homeostasis regulation (Chen *et al.*, 2022; Wang *et al.*, 2020a), osmotic adjustment has rarely been investigated in rice or other crops.

Abscisic acid (ABA) is the major hormone regulating abiotic stress tolerance in plants (Sah *et al.*, 2016). Salt stress causes an increase in ABA accumulation, which improves the signalling of downstream ABA-responsive genes (Cai *et al.*, 2017). Under

salt stress, ABA binds to ABA receptors and interacts with PP2Cs to inhibit their activity and releases SnRK2s from repression (Ma *et al.*, 2009). SnRK2 phosphorylates various AREB (ABA-responsive element-binding protein)/ABF (ABRE-binding factors) transcription factors to regulate abiotic stress (Wang *et al.*, 2020b, 2021). Abscisic acid accumulation is well known as a key osmotic stress response, and it is dependent on the osmotic stress induction of the *NCED3* gene (Fujii *et al.*, 2011). For the biosynthesis of ABA in rice, *OsNCED3* is a gene encoding the key enzyme 9-*cis*-epoxy carotenoid dioxygenase. *OsMADS23* can promote the biosynthesis of endogenous ABA, thereby activating the transcription of the target gene *OsNCED3* (Li *et al.*, 2021). *miR2105* and the kinase *OsSAPK10* co-regulate *OsbZIP86* to mediate drought-induced ABA biosynthesis in rice (Gao *et al.*, 2022). Recently, it has been found that low concentration of ABA is essential for maintaining plant growth, metabolism and development under well-watered conditions (Yoshida *et al.*, 2019). However, little is known about the early regulator of osmotic stress that leads to ABA accumulation under salt stress (Chen *et al.*, 2020a). To elucidate the mechanism underlying osmotic balance and salt tolerance (ST), the functional module participating in ABA biosynthesis under salt stress in rice needs to be investigated.

Please cite this article as: Ge, Y., Chen, G., Cheng, X., Li, C., Tian, Y., Chi, W., Li, J., Dai, Z., Wang, C., Duan, E., Liu, Y., Sun, Z., Li, J., Wang, B., Xu, D., Sun, X., Zhang, H., Zhang, W., Wang, C. and Wan, J. (2024) The superior allele *LEA12^{OR}* in wild rice enhances salt tolerance and yield. *Plant Biotechnol. J.*, <https://doi.org/10.1111/pbi.14419>.

Plenty of potential genomic resources exist in wild rice (Henry, 2022), but there has been no attempt to identify a genetic mechanism of ST from wild rice. In this study, we identified a superior allele of *LEA12^{OR}*, encoding a late embryogenesis abundant (LEA) protein from *Oryza rufipogon* Griff., as a novel component of ABA biosynthesis. *LEA12^{OR}* maintains the kinase stability of OsSAPK10 and promotes *OsNCED3* expression under salt stress. The natural variation in the coding region of *LEA12* in *Oryza rufipogon* Griff. increases the ABA content and results in higher ST. These results are critical for enriching the mechanism underlying osmotic adjustment under salt stress and for deploying natural allelic variation in ST breeding.

Results

Quantitative trait locus mapping and *LEA12^{OR}* identification for salt tolerance

To characterize the potential genetic basis of salt tolerance (ST) in wild rice, we analysed a set of chromosome segment substitution lines (CSSLs) that were generated using *Oryza rufipogon* Griff. as the donor parent and 93-11 (*Oryza sativa* L. subsp. indica) as the recurrent parent. NaCl concentration gradient experiment on different rice varieties showed that 150 mM NaCl was adequate for salt treatment at the seedling stage in laboratory (Figure S1a–c), which was also commonly applied in previous study (Yu *et al.*, 2023). Under hydroponic conditions, *Oryza rufipogon* Griff. showed more ST than 93-11 with a higher survival rate (SR) and shoot fresh weight ratio (SFWR) at 20 days post 150 mM NaCl (Figure S2a–c). In saline fields, *Oryza rufipogon* Griff. exhibited less withering and curling of the leaves at the tillering (four weeks after transplanting) and mature stages (Figure S2d, e). To better distinguish the phenotypes of the CSSLs population under salt stress, we treated the CSSLs with 150 mM NaCl for 15 days and measured the ST-associated traits SR and SFWR. The CSSLs that were extremely sensitive and tolerant to salt stress are displayed in Figure S3a. The SR and SFWR values of the population were continuously distributed (Figure S3b,c).

We constructed a high-density single-nucleotide polymorphism (SNP) linkage map using genotyping-by-sequencing (GBS) and detected 32 249 SNPs throughout the genome of *Oryza rufipogon* Griff. Next, a genome-wide quantitative trait locus (QTL) analysis of ST-associated traits was performed. We identified eight QTLs (Figure 1a; Table S1). The major QTLs *qSR5* and *qSFWR5* were detected with a logarithm of odds (LOD) score of 12.9 in a 397.82 kb region and a LOD score of 8.8 in a 200.3 kb region, respectively, on chromosome 5 (Chr. 5) (Figure 1a,b; Table S1). *qSR5* contains 63.77 kb overlapped with *qSFWR5* (Figure 1b).

We previously designed a genome-wide association study (GWAS)-based strategy to explore and prioritize candidate genes underlying nitrogen use efficiency (NUE) and ST-related traits followed by complementation validation experiments (Tang *et al.*, 2019; Yu *et al.*, 2023). Here, linkage disequilibrium (LD) analysis of the region which contains the two major QTLs indicated that an LD with 34.72 kb contains four open reading frames (ORFs) (Figure 1b, Table S2). *ORF2*, *ORF3* and *ORF4* were induced after salt treatment, of which *ORF4* was induced with the highest sensitivity (Figure 1c). SNP annotation showed missense mutations only in *ORF4* (Table S3). Also, *ORF4* was located on the overlap 63.77 kb region of the two major QTLs. Therefore, *ORF4*

was isolated as the candidate ST gene and encodes an LEA protein *LEA12*, belonging to the *LEA_3* group according to the annotation from the Rice Genome Annotation Project (RAP) database (<https://rapdb.dna.affrc.go.jp/>).

LEA12^{OR} confers salt tolerance in rice

To characterize the function of *LEA12^{OR}* under salt stress, we compared the ST of near-isogenic line (NIL) carrying *LEA12* from *Oryza rufipogon* Griff. (NIL-*LEA12^{OR}*) with 93-11. At 20 days post 150 mM NaCl treatment, the NIL-*LEA12^{OR}* plants showed higher SR and SFWR than 93-11 (Figure 1d–f), suggesting the effects of *qSR5* and *qSFWR5* harbouring *LEA12^{OR}* regulated ST in rice. Then, we obtained *LEA12* knockout plants in the cultivar Nipponbare background using the CRISPR/Cas9 system (Figure S4a). At 10 days post 150 mM NaCl treatment, the SR and SFWR of the *LEA12* knockout plants (*lea12-1*, *lea12-2*) were measured and compared with wild-type Nipponbare (Nip). *lea12-1* and *lea12-2* showed salt sensitivity compared with Nip (Figure S4b–d). This result suggests that *LEA12* acts as a positive regulatory factor conferring ST.

To further confirm the positive regulatory role of *LEA12* in ST, we obtained an *LEA12* tilling mutant (*lea12*) in the cultivar Zhonghua11 (ZH11) background with a single SNP in the coding sequence of *LEA12* (Figure S5a) for ST evaluation. Consistent with the *LEA12* knockout plants, the SR and SFWR of *lea12* mutants were significantly lower than ZH11 at 10 days post salt treatment (Figure S5b–d). These results further indicated that *LEA12* played a positive regulatory role in rice ST. We transformed *LEA12^{OR}* driven by its native promoter into *lea12* (Figure S5a) and found that the complementary plants (Com) restored the salt-sensitive phenotype of the *lea12* mutants (Figure S5b–d). Therefore, we concluded that *LEA12^{OR}* conferred ST in rice.

Natural variation in the coding sequence of *LEA12* affects salt tolerance

To study the natural variations of *LEA12*, the promoter and coding sequence (CDS) of *LEA12^{OR}* (*LEA12* from *Oryza rufipogon* Griff.) and *LEA12⁹³⁻¹¹* (*LEA12* from 93-11) were sequenced. Sequence analysis revealed 26 alterations in the promoters and a 307th SNP variation in the CDS between *LEA12^{OR}* and *LEA12⁹³⁻¹¹* (Figure S6a). We tested the activities of the two promoters by determining the luciferase activities driven by these two promoters (Figure S6b–c), showing no difference between the activities of the two promoters. Meanwhile, the expression levels of *LEA12* were similar between 93 and 11 and *Oryza rufipogon* Griff. both under normal conditions and salt stress (Figure S6d), indicating that the variations in the promoter did not influence the expression of *LEA12*.

The 307th SNP in the CDS led to an alteration from leucine (L) in 93-11 to valine (V) in *Oryza rufipogon* Griff. (Figure S6a). We found no difference in the subcellular localizations (Figure S7a, b) of the two haplotype proteins or their three-dimensional structures using SWISS-MODEL (<https://swissmodel.expasy.org/interactive>) (Figure S7c). However, haplotype analysis of *LEA12^{OR}* and *LEA12⁹³⁻¹¹* exhibited significantly different SR and SFWR using the CSSLs population, and the elite allele was derived from *Oryza rufipogon* Griff. (Figure S7d,e).

To compare the function of the coding sequence of the two haplotypes, we constructed two haplotypes overexpression plants driven by the *Ubiquitin* promoter in the *lea12-1* background. Phenotypes of the overexpression plants were observed at 10 days

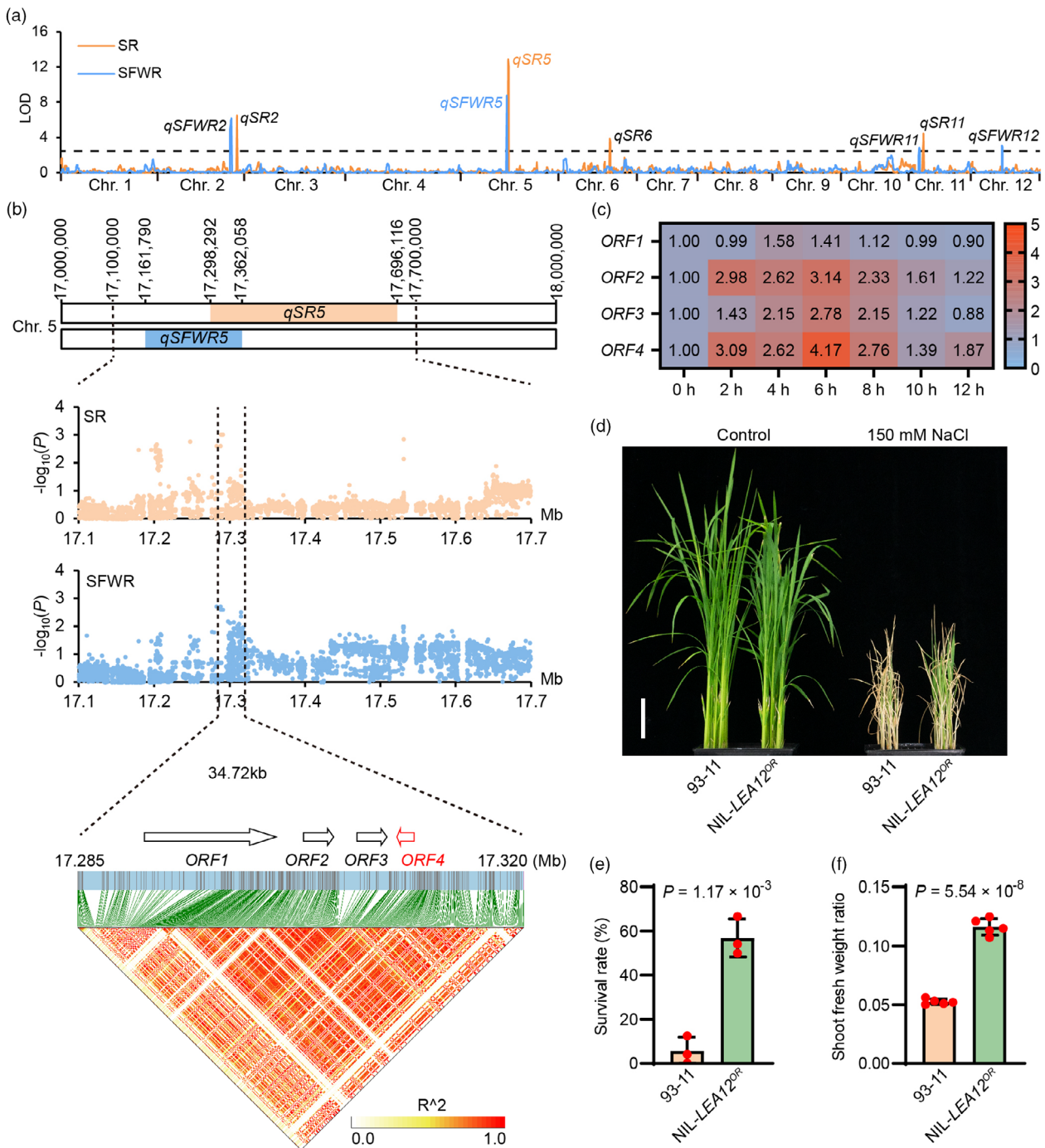


Figure 1 Identification and functional validation of *LEA12^{OR}*. (a) Distribution of the eight ST-related QTLs on chromosomes in rice. The orange line represents the LOD score of survival rate (SR). The blue line represents the LOD score of shoot fresh weight ratio (SFWR). The dotted line represents a LOD threshold value of 2.5. (b) Location of the two major QTLs (*qSR5* and *qSFWR5*) on Chr. 5 (top), local Manhattan plot surrounding the two major QTLs (middle) and LD heatmap surrounding the peak included in the two major QTLs (bottom). (c) Relative expression of the four *ORFs* located in the LD on Chr5 in Nipponbare over time after treated with 150 mM NaCl. Data are means \pm SD ($n = 3$). *ACTIN1* was used as an internal reference. (d) Phenotypes of 93-11 and near-isogenic line (NIL-*LEA12^{OR}*) plants under normal conditions (left) and 150 mM NaCl (right) for 20 days. The scale represents 5 cm. (e) SR of 93-11 and NIL-*LEA12^{OR}* under normal conditions and 150 mM NaCl for 20 days, data are means \pm SD ($n = 3$, each replicate contains 24 plants). (f) SFWR of 93-11 and NIL-*LEA12^{OR}* under normal conditions and 150 mM NaCl for 20 days, data are means \pm SD ($n = 5$). Significant differences in (e) and (f) were determined by Student's *t*-test.

post salt treatment. Obviously, compared with the *lea12-1* plants and Nip, the *LEA12^{OR}* overexpression plants (*lea12-1/OE-OR#1*, *lea12-1/OE-OR#2*) showed stronger ST with less leaf wilting and

blight, a higher SR, and a greater SFWR, whereas *LEA12⁹³⁻¹¹* overexpression plants (*lea12-1/OE-93-11#1*, *lea12-1/OE-93-11#2*) showed the similar SR and SFWR as *lea12-1* (Figure 2a–c).

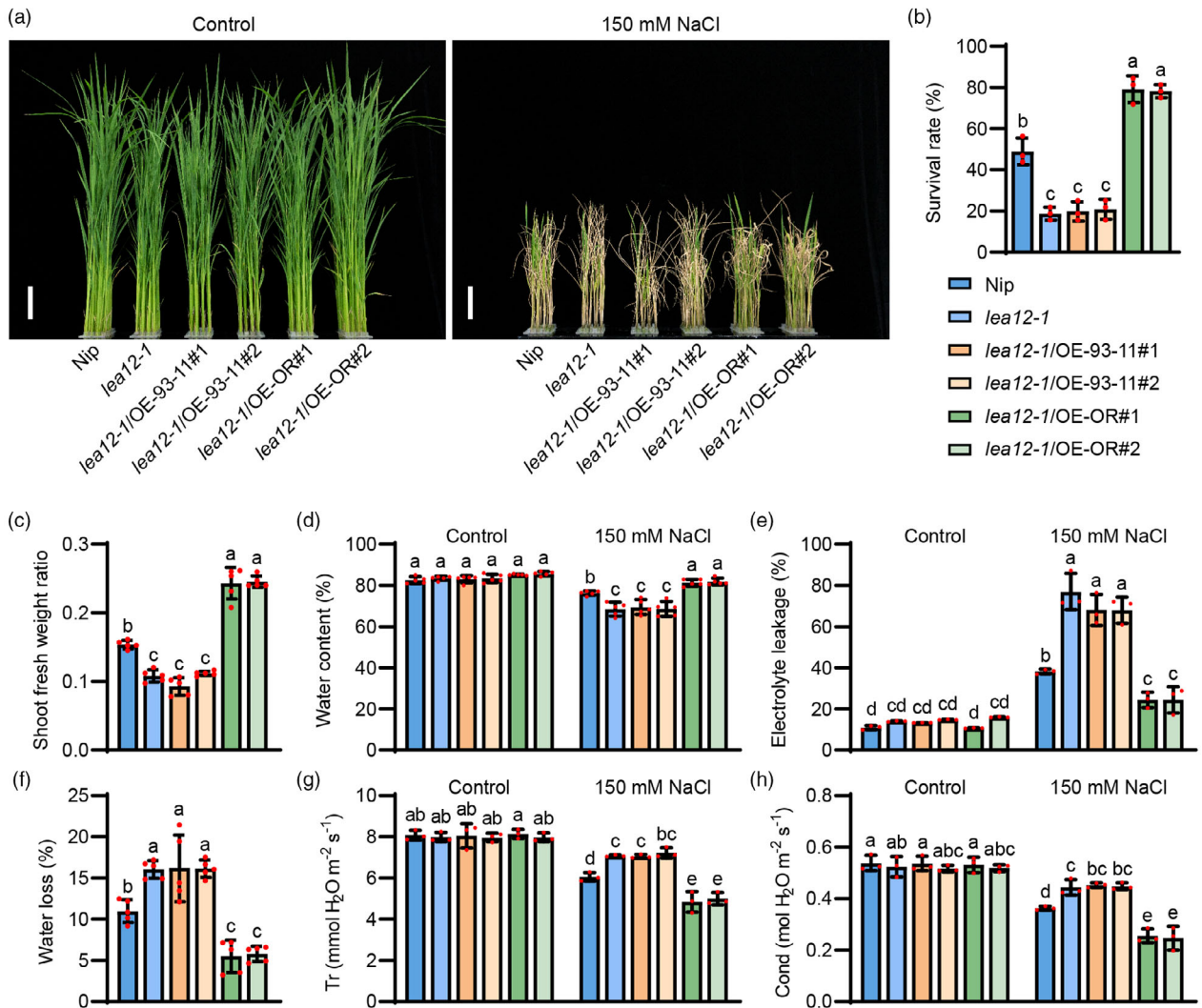


Figure 2 $LEA12^{OR}$, but not $LEA12^{93-11}$, confers ST in rice by osmotic adjustment. (a) Phenotypes of WT Nipponbare (Nip), $LEA12$ knock out ($lea12-1$), $LEA12^{93-11}$ and $LEA12^{OR}$ overexpression plants in $lea12-1$ background ($lea12-1/OE-93-11\#1$, $lea12-1/OE-93-11\#2$, $lea12-1/OE-OR\#1$, $lea12-1/OE-OR\#2$) under 150 mM NaCl for 10 days. The scales represent 5 cm. (b) SR of Nip, $lea12-1$, $lea12-1/OE-93-11\#1$, $lea12-1/OE-93-11\#2$, $lea12-1/OE-OR\#1$, $lea12-1/OE-OR\#2$ under 150 mM NaCl for 10 days, data are means \pm SD ($n = 3$, each replicate contains 32 plants). (c) SFWR of Nip, $lea12-1$, $lea12-1/OE-93-11\#1$, $lea12-1/OE-93-11\#2$, $lea12-1/OE-OR\#1$, $lea12-1/OE-OR\#2$ under 150 mM NaCl for 10 days. (d) Water content (%) of Nip, $lea12-1$, $lea12-1/OE-93-11\#1$, $lea12-1/OE-93-11\#2$, $lea12-1/OE-OR\#1$, $lea12-1/OE-OR\#2$ under 150 mM NaCl for 10 days. (e) Electrolyte leakage (%) of Nip, $lea12-1$, $lea12-1/OE-93-11\#1$, $lea12-1/OE-93-11\#2$, $lea12-1/OE-OR\#1$, $lea12-1/OE-OR\#2$ under 150 mM NaCl for 12 h. (f) Water loss (%) of Nip, $lea12-1$, $lea12-1/OE-93-11\#1$, $lea12-1/OE-93-11\#2$, $lea12-1/OE-OR\#1$, $lea12-1/OE-OR\#2$ under 150 mM NaCl for 10 days. (g) Stomatal conductances (Cond) Nip, $lea12-1$, $lea12-1/OE-93-11\#1$, $lea12-1/OE-93-11\#2$, $lea12-1/OE-OR\#1$, $lea12-1/OE-OR\#2$ under 150 mM NaCl for 48 h. (h) Transpiration rates (Tr) of Nip, $lea12-1$, $lea12-1/OE-93-11\#1$, $lea12-1/OE-93-11\#2$, $lea12-1/OE-OR\#1$, $lea12-1/OE-OR\#2$ under 150 mM NaCl for 48 h. Data in (e, g, h) are means \pm SD ($n = 3$). Data in (c, d, f) are means \pm SD ($n = 5$). Different letters in (b–h) indicate significant differences ($P < 0.05$, one-way ANOVA, Tukey's HSD test).

$LEA12^{OR}$ participates in osmotic adjustment under salt stress

LEA is primarily involved in water-related abiotic stress (Hernandez-Sanchez *et al.*, 2022), so we speculate $LEA12^{OR}$ participates in ST through osmotic adjustment. To verify the role of $LEA12^{OR}$ in osmotic adjustment, we measured the osmotic adjustment-related traits and found $lea12-1$ and $LEA12^{93-11}$ overexpression plants showed lower water content, stomatal conductance and transpiration rate, higher electrolyte leakage and water loss, compared with Nip. $LEA12^{OR}$ overexpression plants showed higher water content, stomatal conductance and

transpiration rate, lower electrolyte leakage and water loss, compared with Nip (Figure 2d–h). In addition, the NIL- $LEA12^{OR}$ showed higher water content, lower electrolyte leakage and water loss than 93-11 (Figure S8a–c). To exclude the effects of ionic and oxidative stresses, we detected key genes that positively regulate salt tolerance in rice and found that osmotic-stress-related genes *SWEET15* and *P5CS1* were down-regulated in $lea12-1$ plants, while the expressions of ionic-stress and oxidative-stress-related genes were not down-regulated (Figure S9). In addition, there was no significant difference in Na^+ and K^+ contents between the near-isogenic line NIL- $LEA12^{OR}$ and 93-11 after two days of salt treatment (Figure S10). These

results indicated that *LEA12^{OR}* mainly regulated osmotic stress response under salt stress.

Consistent with the trend of salt treatment, the *lea12-1* and *LEA12⁹³⁻¹¹* overexpression plants showed drought sensitive with lower SFWR and SR at seven days post drought treatment compared with Nip. The *LEA12^{OR}* overexpression plants showed higher SR and SFWR compared with Nip, *lea12-1* and *LEA12⁹³⁻¹¹* overexpression plants with watering withheld for seven days (Figure S11a–c). This result further indicated the involvement of *LEA12^{OR}* in osmotic adjustment.

LEA12^{OR} interacts with OsSAPK10 to confer salt resistance

To investigate how *LEA12^{OR}* participated in the regulatory mechanism promoting ST, we conducted yeast two-hybrid library screening and found an SNF1-related protein kinase, OsSAPK10, in these yeast clones (Table S4). Under drought stress, OsSAPK10 regulated the expression of *OsNCED3*, a critical enzyme 9-*cis*-epoxy carotenoid dioxygenase in the ABA biosynthesis pathway (Gao *et al.*, 2022).

To confirm the interaction between *LEA12* and OsSAPK10 *in vivo*, we observed the organizational expression patterns of *LEA12* and *OsSAPK10*, showing high relative expressions in leaf (Figure S12a, b). *LEA12* and *OsSAPK10* also showed the similar salt-induced expression pattern in shoot (Figure S12c). Further *in situ* hybridization assay exhibited their colocalization signal in rice leaf, especially in epidermal cells (Figure S12d).

To further validate the protein interaction between *LEA12* and OsSAPK10, a co-immunoprecipitation (Co-IP) assay in *Nicotiana benthamiana* confirmed that FLAG-*LEA12^{OR}* and FLAG-*LEA12⁹³⁻¹¹* could be co-immunoprecipitated with OsSAPK10-GFP, but not an empty GFP protein, using anti-GFP beads (Figure 3a). Furthermore, a pull-down assay was conducted. We found either GST-*LEA12^{OR}* or GST-*LEA12⁹³⁻¹¹* was pulled down by MBP-OsSAPK10 (Figure 3b). In addition, a bimolecular fluorescence complementation (BiFC) assay showed both p2YN-*LEA12^{OR}* and p2YN-*LEA12⁹³⁻¹¹* interacted with p2YC-OsSAPK10. The interaction fluorescence was appeared in nucleus and cytoplasm (Figure 3c).

Notably, *LEA12^{OR}* and *LEA12⁹³⁻¹¹* overexpression plants exhibited different ST phenotypes. Consistent with the phenotypical differences under salt stress, the BiFC assay showed stronger fluorescence intensity in the combination of *LEA12^{OR}*-OsSAPK10 than that of *LEA12⁹³⁻¹¹*-OsSAPK10 (Figure 3c). Based on this, we speculated that the interaction between *LEA12^{OR}* and OsSAPK10 is stronger than that between *LEA12⁹³⁻¹¹* and OsSAPK10. To verify this, we next conducted a luciferase complementation imaging (LCI) assay. Co-expression of cLUC-*LEA12^{OR}* and OsSAPK10-nLUC produced stronger luciferase signals than the co-expression of cLUC-*LEA12⁹³⁻¹¹* and OsSAPK10-nLUC (Figure 3d,e; Figure S13). The microscale thermophoresis (MST) assay revealed that *LEA12^{OR}* bound to OsSAPK10 protein more strongly than *LEA12⁹³⁻¹¹*, with a seventh K_d value (Figure 3f). These results suggested that *LEA12^{OR}*, as the elite haplotype, enhanced ST through stronger interaction with OsSAPK10 in rice.

To further explore the genetic relation between *LEA12* and OsSAPK10, we constructed OsSAPK10 knockout plants in the Nip and *lea12-1* background (Figure 4a) and found that *lea12-1/ossapk10* double knockout plants showed similar SR and SFWR to *lea12-1* or *ossapk10* plants at 10 days post NaCl treatment (Figure 4b–d), indicating that *LEA12* and OsSAPK10 genetically interact with each other under salt stress. Also, *lea12-1*, *ossapk10* and *lea12-1 ossapk10* showed the lower water content, lower

electrolyte leakage and higher water loss compared with Nip, consistent with their phenotypes (Figure 4e–g). As OsSAPK10 played a key role in ABA biosynthesis under drought stress (Gao *et al.*, 2022), we speculated that *LEA12^{OR}* and OsSAPK10 regulated ABA biosynthesis under salt stress. As expected, overexpression of *LEA12^{OR}* improved ABA content under salt stress, while knockout of *LEA12* or OsSAPK10 reduced the ABA content (Figure 4h).

LEA12^{OR} maintains OsSAPK10 stability under salt stress

It was reported that an LEA protein MtCAS31 protected MtLb120-1 (Li *et al.*, 2018), so we speculated that *LEA12^{OR}* could protect the OsSAPK10 protein from degradation under salt stress. First, an *in vitro* cell-free degradation assay was carried out, which indicated that the MBP-OsSAPK10 protein was degraded gradually over time when incubated with the total protein extracts from the 93-11 (Figure 5a). Interestingly, the degradation was relieved when GST-*LEA12^{OR}* was added, but not GST-*LEA12⁹³⁻¹¹* (Figure 5a). Furthermore, MBP-OsSAPK10 was more rapidly degraded in the total protein extracted from 93-11 than that from NIL-*LEA12^{OR}* (Figure 5b). In rice plants, the OsSAPK10-GFP was more rapidly degraded in the *lea12-1* than that in Nip when NaCl was applied (Figure 5c). Considering that the ubiquitin–proteasome system is the typical pathway for protein degradation in eukaryotic cells, we added MG132 (a proteasome inhibitor) to the nutrient solution and found that MG132 inhibited OsSAPK10 degradation (Figure 5c). To further verify the protective function of *LEA12^{OR}* on OsSAPK10 *in vivo*, we co-transferred *OsSAPK10-GFP* with *FLAG-LEA12^{OR}*, *FLAG-LEA12⁹³⁻¹¹* or empty *FLAG* into tobacco epidermal cells. Under NaCl treatment, fewer GFP fluorescence was observed and fewer OsSAPK10-GFP protein was detected indicating that OsSAPK10-GFP was degraded when the absence of *FLAG-LEA12^{OR}*, and the rate of degradation was reduced when MG132 was added (Figure 5d–f). We therefore concluded that *LEA12^{OR}* regulated OsSAPK10 protein stability.

It was reported that OsbZIP86, phosphorylated by OsSAPK10, regulated *OsNCED3* expression (Gao *et al.*, 2022). Our *in vitro* phosphorylation assay showed that MBP-OsbZIP86 was phosphorylated by GST-OsSAPK10, especially when the presence of GST-*LEA12^{OR}* (Figure S14). This implied its protective effect. Then, we detected the expression level of *OsNCED3* in the *lea12-1* and overexpression plants, and found that *OsNCED3* expression was reduced in *lea12-1* and *LEA12⁹³⁻¹¹* overexpression plants and increased in *LEA12^{OR}* overexpression plants compared with Nip under salt stress (Figure S15). These results established the *LEA12^{OR}*-OsSAPK10-OsbZIP86-OsNCED3 functional module that conferred ST by promoting ABA synthesis, suggesting that *LEA12^{OR}* enhanced ST as the elite haplotype and thus has breeding potential for ST improvement.

Potential breeding of *LEA12^{OR}*

To explore the breeding potential of *LEA12^{OR}*, we analysed the variation of *LEA12* in the rice 3K population. Among the five haplotypes of *LEA12*, HapC is an ancient haplotype from *Oryza rufipogon* Griff. which the other haplotypes, including HapE (93-11) evolved from (Figure S16a). We calculated the nucleotide diversity within an ~120 kb interval surrounding the *LEA12* gene and observed an interval of ~40 kb surrounding *LEA12* with significantly reduced nucleotide diversity in indica, subtropical and temperate subpopulations relative to *Oryza rufipogon* Griff. (Figure S16b). This selective sweep signal indicated low nucleotide diversity in the *LEA12* region due to artificial selection in rice.

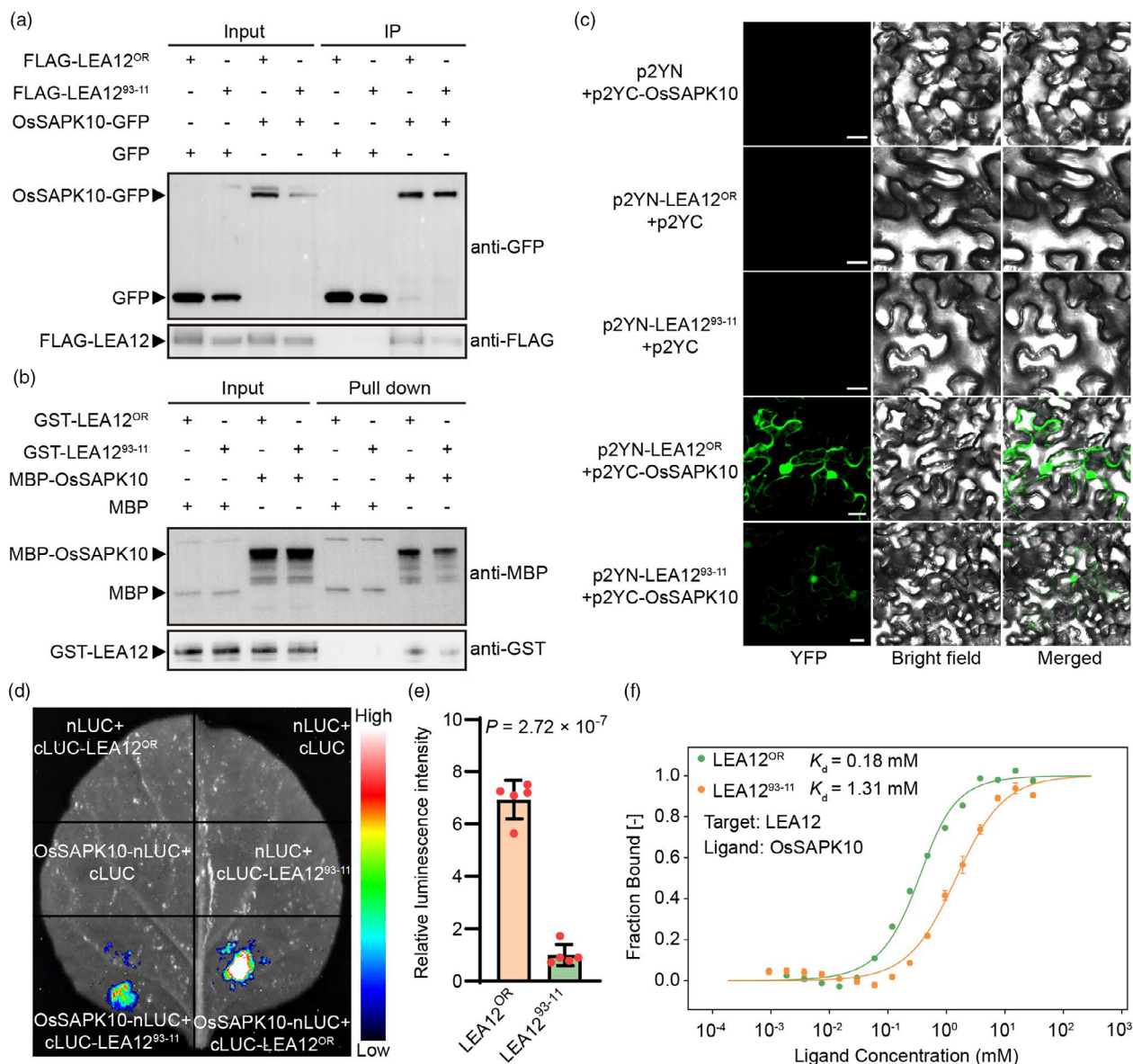


Figure 3 LEA12 interacts with OsSAPK10 in vivo and in vitro. (a) In vivo Co-IP assay in *Nicotiana benthamiana*. FLAG-LEA12^{OR} or FLAG-LEA12⁹³⁻¹¹ was co-immunoprecipitated with OsSAPK10-GFP, but not co-immunoprecipitated with the empty GFP protein, using anti-GFP beads. Black triangles indicate the position of the strip. (b) In vitro pull-down assay of MBP-OsSAPK10 with GST-LEA12^{OR} or GST-LEA12⁹³⁻¹¹ using MBP-Sepharose Dextrin Agarose Resin, empty MBP protein was used as control. Black triangles indicate the position of the strip. (c) BiFC assay of p2YN-LEA12^{OR} or p2YN-LEA12⁹³⁻¹¹ with p2YC-OsSAPK10, p2YN and p2YC were used as negative control. The scales represent 20 μm. (d, e) The LCI assay of both cLUC-LEA12⁹³⁻¹¹ and cLUC-LEA12^{OR} with OsSAPK10-nLUC, empty cLUC and nLUC were used as control. (d) The pseudo colour image of luminescence. (e) The relative luminescence intensity. Data are means ± SD (n = 5). Significant differences were determined by Student's *t*-test. (f) MST assay of LEA12⁹³⁻¹¹ or LEA12^{OR} protein binding affinity with OsSAPK10 protein.

Meanwhile, the superior allele *LEA12^{OR}* presented different distribution proportions in subpopulations and regions, with a high proportion of distribution in japonica and areas with more saline-alkali lands (Figure S16c, d). These results imply that *LEA12^{OR}* plays an important role in the artificial selection.

Furthermore, field experiments were performed in a saline field. We found that NIL-*LEA12^{OR}* showed more ST than 93-11 in saline field (Figure 6a). NIL-*LEA12^{OR}* improved yield per plant with higher effective panicle number, grain number per panicle, seed setting rate than 93-11, but the plant height, grain length, grain

width, or 1000-grain weight were not affected (Figure 6b–j). By the way, *LEA12^{OR}* overexpression plants also exhibited increased yield per plant in saline fields than the wild type (Figure S17a, b). These results demonstrated that *LEA12^{OR}* improved ST and yield under salt stress.

Taken together, *LEA12^{OR}*, encoding an LEA protein from the wild rice *Oryza rufipogon* Griff., improved osmotic adjustment and increased yield under salt stress. *LEA12^{OR}* maintains OsSAPK10 kinase stability, and *LEA12^{OR}*-OsSAPK10-OsbZIP86-OsNCED3 formed a novel functional module participating in ABA

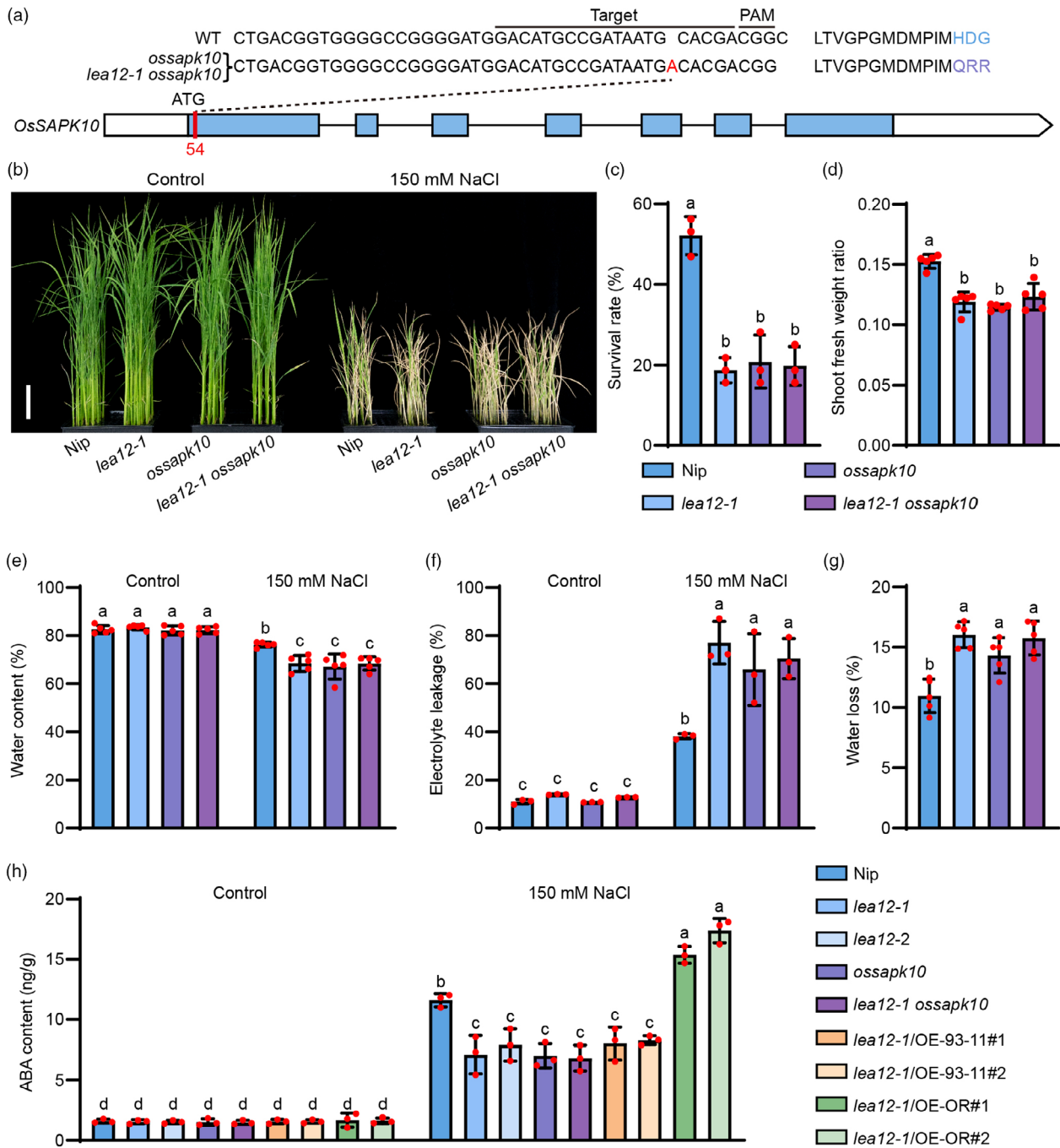


Figure 4 *LEA12* genetically interacts with *OsSAPK10* and affects ABA content in rice. (a) Insertion of a 54th adenine led to frameshift mutation. (b) Phenotypes of Nip, *lea12-1*, *ossapk10*, *lea12-1 ossapk10* under 150 mM NaCl for 10 days, the scale represents 5 cm. (c) SR of Nip, *lea12-1*, *ossapk10*, *lea12-1 ossapk10* under 150 mM NaCl for 10 days. (d) SFWR of Nip, *lea12-1*, *ossapk10*, *lea12-1 ossapk10* under 150 mM NaCl for 10 days. (e) Water content (%) of Nip, *lea12-1*, *ossapk10*, *lea12-1 ossapk10* under 150 mM NaCl for 10 days. (f) Electrolyte leakage (%) of Nip, *lea12-1*, *ossapk10*, *lea12-1 ossapk10* under 150 mM NaCl for 10 days. (g) Water loss (%) of Nip, *lea12-1*, *ossapk10*, *lea12-1 ossapk10* under 150 mM NaCl for 10 days. (h) ABA contents of Nip, *LEA12-cr*, *ossapk10*, *lea12-1 ossapk10* and *LEA12* overexpression plants. Data in (c, f, h) are means \pm SD ($n = 3$). Data in (d, e, g) are means \pm SD ($n = 5$). Different letters in (c–h) indicate significant differences ($P < 0.05$, one-way ANOVA, Tukey's HSD test).

biosynthesis in rice (Figure 7). Our results elucidate the mechanism of osmotic adjustment in ST due to enhanced ABA biosynthesis and provide new avenues for improving ST and yield via the deployment of the elite allele of *LEA12^{OR}* through molecular breeding and genome editing.

Discussion

Salinity stress progressively reduces plant productivity and has negative impacts on sustainable agriculture. Over the last decade, breakthrough discoveries of natural variation in Na^+ transporters

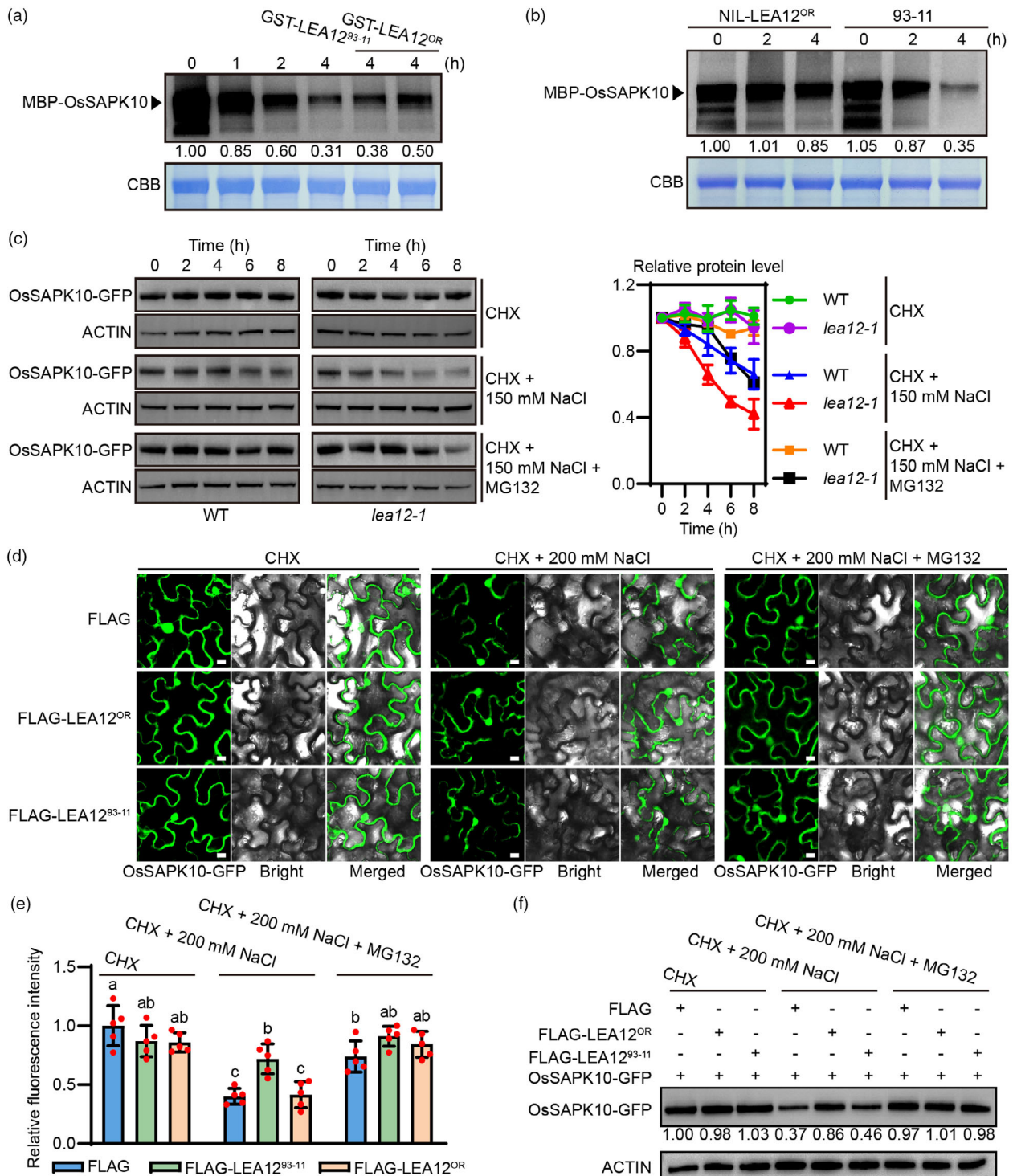


Figure 5 LEA12^{OR} maintains OsSAPK10 protein stability. (a) Cell-free degradation analysis of the recombinant MBP-OsSAPK10 protein. The total protein extracted from 93-11 plants was incubated with MBP-OsSAPK10 combined with GST-LEA12⁹³⁻¹¹ or GST-LEA12^{OR}. Coomassie brilliant blue (CBB) staining of Rubisco was shown as a loading control. (b) Cell-free degradation analysis of the recombinant MBP-OsSAPK10 protein. The total protein extracted from 93-11 or NIL-LEA12^{OR} was incubated with MBP-OsSAPK10. CBB staining of Rubisco was shown as a loading control. (c) OsSAPK10-GFP protein level in WT (*Nip*) and *lea12-1* plants over time under different conditions. ACTIN was used as internal reference. CHX (Sigma, C21865), cycloheximide, a protein biosynthesis inhibitor. MG132 (Sigma, C2211), a proteasome inhibitor. (d-f) OsSAPK10-GFP were co-transferred into tobacco epidermal cells with empty FLAG, FLAG-LEA12^{OR} or FLAG-LEA12⁹³⁻¹¹. Images of OsSAPK10-GFP fluorescence in tobacco epidermal cells under different conditions (e), scales represent 10 μ m. Data of relative fluorescence intensity (f) are means \pm SD ($n = 5$). Different letters indicate significant differences ($P < 0.05$, one-way ANOVA, Tukey's HSD test). The OsSAPK10-GFP protein level under different conditions (g). ACTIN was used as internal reference.

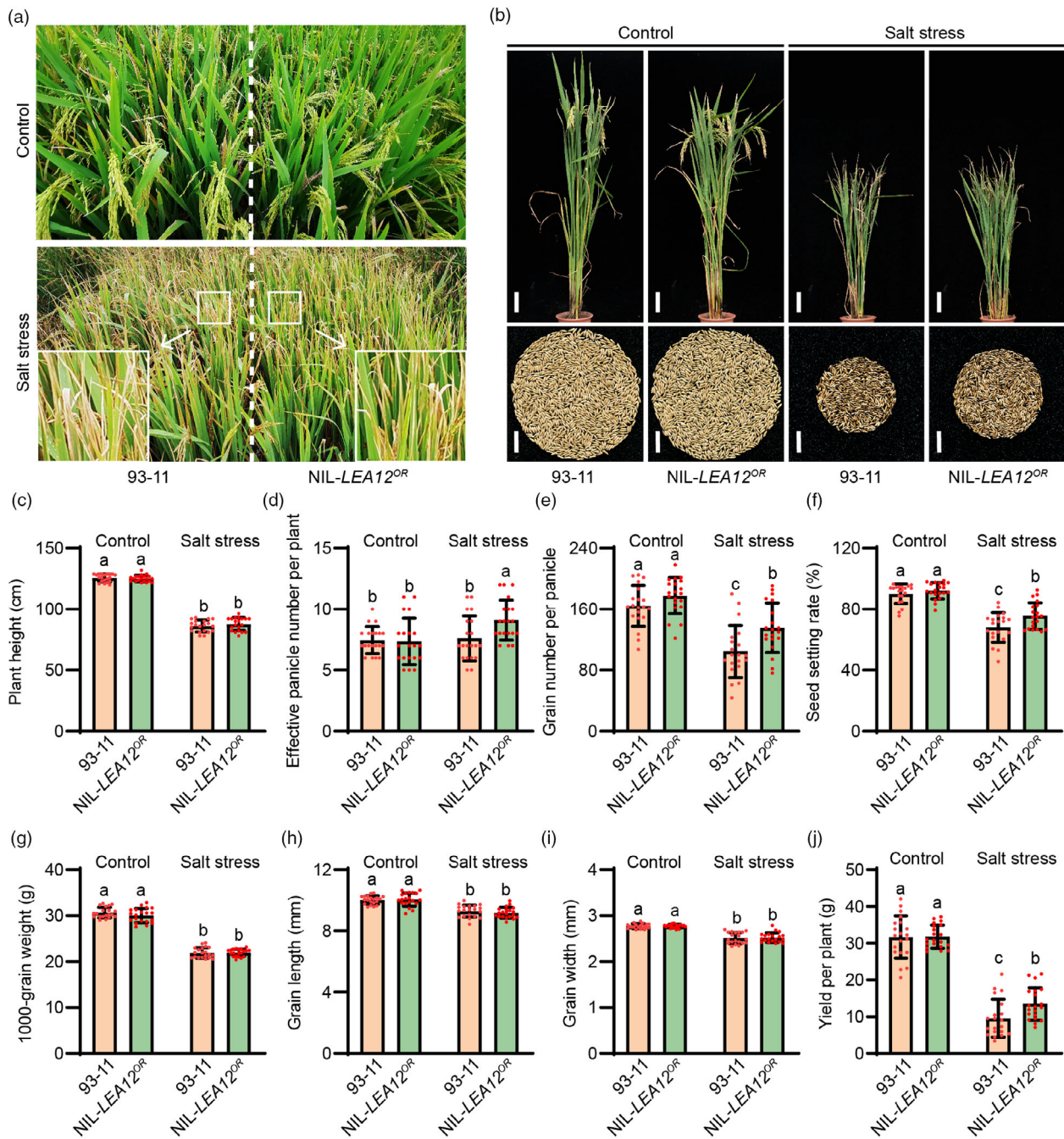


Figure 6 Salt stress phenotypes of 93-11 and NIL-*LEA12^{OR}* plants throughout the life cycle. (a) Field photographs were taken at mature stage in Lianyungang, China, 2023. (b) Plant photographs were taken at mature stage, the scales represent 10 cm. Grains were taken after harvest, the scales represent 3 cm. (c) Plant height (cm). (d) Effective panicle number per plant. (e) Grain number per panicle. (f) Seed setting rate (%). (g) 1000-grain weight (g). (h) Grain length (mm). (i) Grain width (mm). (j) Yield per plant (g). Data in (c–j) are means \pm SD ($n = 20$), different letters indicate significant differences ($P < 0.05$, one-way ANOVA, Tukey's HSD test).

underlying ST, such as *SKC1*, have been made in rice (Ren *et al.*, 2005). However, the natural variation of key genes underlying osmotic adjustment and ABA biosynthesis remains largely unexplored in rice. The urgency in addressing this is heightened by concerns around food security, water availability and climate change. In this study, through QTL analysis and LD mapping, we isolated novel ST-associated QTLs from the wild rice *Oryza rufipogon* Griff., which harbours the *LEA12^{OR}* gene

encoding an LEA protein. *LEA12^{OR}* improves osmotic adjustment and increases yield under salt stress. Mechanistically, *LEA12^{OR}*, as the early regulator of the *LEA12^{OR}-OsSAPK10-OsZIP86-OsNCED3* functional module, maintains the kinase stability of *OssSAPK10* under salt stress, and thereby confers ST by promoting ABA biosynthesis and accumulation in rice.

ABA is the most important hormone of abiotic stress tolerance in plants (Zelm *et al.*, 2020). Salt stress causes an increase in ABA

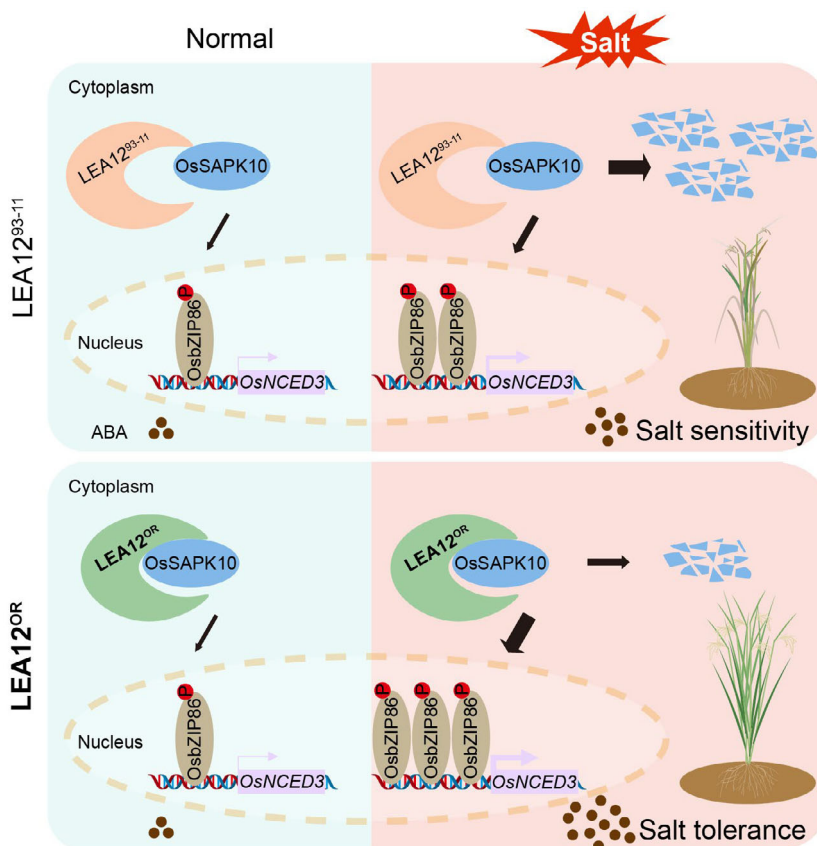


Figure 7 Working model of *LEA12^{OR}* in rice. *LEA12^{OR}*, from the wild rice *Oryza rufipogon* Griff., encoding an LEA protein. *LEA12^{OR}*, but not *LEA12⁹³⁻¹¹* maintains OsSAPK10 protein stability, improves osmotic adjustment and increases yield under salt stress. *LEA12^{OR}*-OsSAPK10-OsbZIP86-OsNCED3 forms a novel functional module participating in ABA biosynthesis under salt stress in rice.

accumulation (Welsch *et al.*, 2008). Abscisic acid accumulation is dependent on the osmotic stress induction of the *NCED3* gene that is responsible for the biosynthesis of ABA (Fujii *et al.*, 2011). The kinase OsSAPK10-regulates OsbZIP86 to mediate drought-induced ABA biosynthesis in rice (Gao *et al.*, 2022). ABA can regulate stomatal closure and salt stress-responsive gene expression (Chen *et al.*, 2020b). Together with these findings, we have identified *LEA12^{OR}* as the early regulator of ABA biosynthesis and enriched the mechanism underlying salt tolerance through osmotic adjustment.

The LEA proteins were first discovered in cotton embryos and were widespread in eukaryotes (Li *et al.*, 2020; Liang *et al.*, 2019). In *Medicago truncatula*, dehydrin MtCAS31 has been shown to protect leghemoglobin under drought stress (Xie *et al.*, 2012) and works as a cargo receptor in the drought-induced autophagic degradation of MtPIP2;7 (Li *et al.*, 2020). LEAs were reported to be involved in various abiotic stresses, such as drought (Liang *et al.*, 2019; Xie *et al.*, 2012), salt (Ganguly *et al.*, 2012), and cold (Candat *et al.*, 2014). In this study, we investigated the mechanisms of osmotic adjustment by LEA protein in ST. Moreover, we discovered the genetic variation of LEAs and the molecular mechanism underlying the regulatory pathway of LEAs (Figure 7).

Intriguingly, the expression of stress-activated protein kinase OsSAPK10 was upregulated under salt stress (Figure S12c), but the protein level was reduced without *LEA12^{OR}* under salt stress in this study (Figure 5d–f). We provided evidences that *LEA12^{OR}* maintained the protein stability and kinase activity of OsSAPK10 through stronger interaction with OsSAPK10 under salt stress. The 307th SNP in the CDS of *LEA12* influenced the interaction with OsSAPK10 and led to different ST phenotypes (Figure 2a–c; Figure 3d–f). We found that *LEA12* formed five haplotype groups

(HapA–HapE) in the rice 3 K population (Wang *et al.*, 2018) (Figure S16a) with four SNPs, including the 307th one. The superior allele of *LEA12^{OR}* has undergone artificial selection for salt tolerance and yield enhancement, and provides a new avenue to improve ST and yield via the deployment of *LEA12^{OR}* in current rice through molecular breeding and genome editing. This study addresses a long-standing question of how crops adapt to salt stress through maintaining osmotic adjustment.

To breed and cultivate high-yield and high-quality rice varieties with ST, it is crucial to explore the mechanisms underlying ST in rice. However, little progress has been made in developing salt-tolerant rice varieties, probably due to the limited availability of elite alleles for crop breeding. Detecting salt-tolerant genes within currently cultivated crops remains a challenge due to the relatively low levels of genetic diversity. In this study, we successfully re-applied the elite allele of *LEA12^{OR}* in wild rice for ST and yield improvement in current rice cultivars.

To determine whether the function of *LEA12* is conserved in other plant species, we assessed the function of the *LEA12* gene in maize using a mutant of B73 *zmlea12* planted in natural saline field with 0.1%–0.2% salinity (Figure S18a). Analysis of the mutant plants showed that *zmlea12* exhibited shorter and lower chlorophyll content than B73 under salt stress but not under normal condition (Figure S18b–d). This result implied that the conserved function of *LEA12* provides the potential to improve ST of other crops.

In summary, developing salt-tolerant crops is critical for sustainable agriculture. We discovered the mechanism underlying osmotic adjustment in ST and highlighted the value of largely underexplored wild germplasm for identifying more elite alleles of high ST that can be deployed in the breeding of ST cultivars.

Experimental procedures

Plant materials, plasmids construction and growth conditions

The seeds of chromosome segment substitution lines (CSSLs) were supplied by the State Key Laboratory of Crop Genetics and Germplasm Enhancement Utilization, Nanjing Agricultural University, China. The tilling mutant *lea12* was supplied by Professor Chunming Liu (School of Advanced Agricultural Sciences, Peking University, China). Maize mutant *zmlea12* was purchased from the following website (<https://elabcaas.cn/memd/public/index.html#/>).

The *LEA12* and *OsSAPK10* knockout vectors were constructed using the CRISPR/Cas9 system. Then, the *LEA12* knockout plasmid was introduced into Nipponbare (Nip) using *Agrobacterium*-mediated transformation to obtain *lea12-1* and *lea12-2* plants. The *OsSAPK10* knockout plasmid was introduced into Nip to obtain *ossapk10* plants and introduced into *lea12-1* to obtain *lea12-1 ossapk10* double mutant plants. Positive plants were confirmed by polymerase chain reaction (PCR) followed by sequencing. All primers used for PCR here and in the following sections are listed in Table S5. To obtain *LEA12* overexpression lines, the full-length CDS of *LEA12^{OR}* and *LEA12⁹³⁻¹¹* were cloned into *pCUBi1390* vector and driven by the maize *Ubiquitin* promoter. The plasmids were transformed into *lea12-1* plant. The CDS of *LEA12^{OR}* with 2 kb promoter were cloned into *pCUBi1390* vector and transformed into *LEA12* to obtain complementary plants. The CDS of *OsSAPK10* was cloned into *pCAMBIA1305* vector and transformed into Nip and *lea12-1* to express *OsSAPK10*-GFP protein.

All rice plants were grown in the chamber (12 h light at 30°C/12 h darkness at 28°C, relative humidity of ~70%) in Nanjing Agricultural University for phenotypic evaluation. For hydroponics experiments, rice seedlings were cultured in Yoshida's nutrient solution (with slight modifications). NaCl was added to the solution at three-leaf stage (14-day-old), and the solution was changed every 2 days. After several days (slightly different depending on the variety), the plants were photographed and the shoot fresh weight ratio (SFWR, shoot fresh weight under salt stress/shoot fresh weight under normal conditions) was determined. The survival rate (SR) was determined after 1 week recovery. For the drought treatment, all plants were grown in nutrient soil, and watering was withheld at the three-leaf stage. One week later, the SFWR was determined and the plants were rewatered. Photographs were taken after 1 week recovery, and the SR was counted simultaneously.

For the field experiment, all plants were planted at Qingkou farm (salt stress, with 0.3%–0.5%, maize with 0.1%–0.2% salt) and Dongxin farm (control), Lianyungang Academy of Agricultural Science, China, in 2023, with three repeats. At mature stage, the plants were photographed and the phenotypes were determined.

QTL analysis and LD mapping

Survival rate and shoot fresh weight ratio were scored for QTL analysis using QTL IciMapping v4.1 software with a threshold LOD of 2.5. Linkage disequilibrium analysis in the QTL regions and haplotype analyses were previously described (Tang *et al.*, 2019).

Quantitative real-time PCR (qRT-PCR)

The total RNA from different tissues was extracted using an RNAprep Pure Plant Kit (TIANGEN). The cDNA for the qRT-PCR was reverse-transcribed from 2 µg of total RNA using the

PrimeScript II Reverse Transcriptase (TaKaRa). The qRT-PCR was performed using a SYBR Premix Ex Taq™ kit (TaKaRa) in a Real-Time PCR machine (Bio-Rad) according to the manufacturer's instructions. The rice *ACTIN1* gene was selected as the internal control.

Subcellular localization

The CDS of *LEA12^{OR}* and *LEA12⁹³⁻¹¹* were cloned into the pAN580 vector to express *LEA12^{OR}*-GFP and *LEA12⁹³⁻¹¹*-GFP fusion protein. All transient expression constructs were separately transformed into rice protoplasts and incubated in the dark at 28°C for 16 h before examination. Green fluorescent protein fluorescence was observed using a confocal laser-scanning microscope (Leica TCS SP8; Leica Microsystems, Wetzlar, Germany).

Measurement of ABA content

The plant materials were treated with 150 mM NaCl for 2 days, following which the shoots were ground to a fine powder in liquid nitrogen. Isopropanol–water–hydrochloric acid mixed extraction solution was added to extract the ABA. The ABA was measured by high-performance liquid chromatography–tandem mass spectrometry (HPLC-MS/MS; Aglient1290, AB SCIEX-6500 Qtrap).

Measurement of water content, electrolyte leakage and water loss

All plants were grown as previously described; shoot fresh weight (SFW), shoot dry weight (SDW) and electrolyte leakage (EL) were measured after treated with 150 mM NaCl for 10 days. Water content (WC) was calculated using the following equation:

$$WC (\%) = (SFW - SDW) / SFW \times 100.$$

Second leaf blade (counting from the new leaf) of three rice seedlings was cut into 1 cm segments and mixed together in test tubes containing 10 mL of ddH₂O. The conductivity of ddH₂O (C0) before adding the leaves, conductivity after adding the leaves and leaving them for 24 h after shaking (C1), and conductivity after boiling in a water bath for 0.5 h (C2) were determined by a conductivity meter (S230, METTLER) and calculated by the following equation: $EL (\%) = (C1 - C0) \div (C2 - C0) \times 100$.

Moisture weight was measured before salt treatment (W1) and 12 h (W2) after salt stress.

$$\text{Water loss (\%)} = (W1 - W2) / W1.$$

Measurement of chlorophyll content

For chlorophyll extraction, 1 g new leaves of B73 and *zmlea12* were extracted with 5 mL 95% ethanol. Chlorophyll contents were determined as previously (Wang *et al.*, 2016).

Measurement of stomatal conductance and transpiration rate

All plants were grown as mentioned above and then treated with 150 mM NaCl for 48 h. The stomatal conductance and transpiration rate were measured using a photosynthesis system (LI-6400XT) at a 1000 µmol m⁻² s⁻¹ light intensity in the chamber.

Measurement of Na⁺ and K⁺ content

NIL-*LEA12^{OR}* and 93-11 plants were grown as mentioned above. Measurement of ion concentration in the rice tissues was performed as described previously (An *et al.*, 2020). In brief,

after 2 days of 150 mM NaCl treatment, the shoots of the rice seedlings were harvested separately, rinsed with deionized water three times, and then dried at 50°C for 1 week. Then, 0.1 g dried samples were digested with 5 mL ultrapure nitric acid at 50°C overnight and then at 120°C for 1 h until no residue remained in the test tube. Ion contents were determined using inductively coupled plasma-optical emission spectroscopy (ICP-OES) (Optima 8000, PerkinElmer).

Pull-down assay

The CDS of *LEA12^{OR}* and *LEA12⁹³⁻¹¹* were cloned into the pGEX-4T-2 vector, and the CDS of *OssSAPK10* was cloned into pMAL-c2X. Then, the vectors were transformed into *E. coli* strain BL21 (DE3) to express fusion protein GST-*LEA12^{OR}*, GST-*LEA12⁹³⁻¹¹* and MBP-*OssSAPK10*. The proteins were purified using amylose agarose beads and glutathione magnetic beads (Solarbio). The fusion proteins were incubated in PBS at 4°C with amylose agarose beads. The antibodies against maltose-binding protein (anti-MBP; 1:5000 dilution) (NEB, Ipswich, MA, USA) or GST (1:5000 dilution; Millipore) and the anti-mouse second antibody (1: 5000 dilution; Abmart, Shanghai, China) were used in this experiment. Western blots were performed using a High-sig ECL Western Blotting Substrate (Tanon, Shanghai, China).

Co-immunoprecipitation (Co-IP) assay

FLAG-LEA12^{OR}, *FLAG-LEA12⁹³⁻¹¹* and *OssSAPK10-GFP* were co-transformed into *N. benthamiana*. Total proteins were then extracted from *N. benthamiana* and incubated with GFP beads for 4 h at 4°C to immunoprecipitate the target protein. The GFP beads were washed with cold lysis/IP buffer (50 mM Tris–MES (pH 8.0), 0.5 M Sucrose, 1 mM MgCl₂, 10 mM EDTA, 5 mM DTT and 0.5% NP-40 (Amresco, E109)) 3–5 times. Before use, a protease inhibitor cocktail was added to the lysis buffer. The beads were boiled with SDS loading buffer at 100°C for 5 min, and western blots were performed. Anti-FLAG (dilution 1:5000, MBL M185-7) and anti-GFP (dilution 1:5000, Abcam) were used in western blot assay.

Bimolecular fluorescence complementation (BiFC) assay

The CDS of *LEA12^{OR}* and *LEA12⁹³⁻¹¹* were cloned into p2YN, and *OssSAPK10* was cloned into the p2YC, forming the YFP^N-*LEA12^{OR}*, YFP^N-*LEA12⁹³⁻¹¹*, YFP^C-*OssSAPK10* fusion proteins. The recombinant BiFC vectors were then co-transformed into *N. benthamiana*. Fluorescence was observed using a confocal laser-scanning microscope after 48 h.

Luciferase complementation imaging (LCI) assays

The full-length CDS of *LEA12^{OR}* and *LEA12⁹³⁻¹¹* were cloned into the cLUC, and *OssSAPK10* was cloned into nLUC. The recombinant vectors were then co-transformed into *N. benthamiana*. Luciferase activity and protein level were detected after 48 h.

Microscale thermophoresis (MST) assay

The GST-*LEA12^{OR}* and GST-*LEA12⁹³⁻¹¹* proteins were used as targets, and MBP-*OssSAPK10* was used as ligand. Prepare a serial dilution of the diluted MBP-*OssSAPK10* using buffer PBST. Then, the dilutions were incubated with GST-*LEA12^{OR}* or GST-*LEA12⁹³⁻¹¹* for 10 min, following which the samples were analysed by Monolith NT.115 (NanoTemper Technologies) at 25°C, 30% MST power, and 20% LED power using hydrophobic capillaries (Polymicro Technologies). The results are displayed with three biological replicates and were analysed by MO. Affinity Analysis software (V2.2.4).

Cell-free degradation

The cell-free degradation assay was performed as previously described (Wang *et al.*, 2009). The total protein was extracted from 93-11 and NIL-*LEA12^{OR}* by lysis buffer (50 mM Tris–MES (pH 8.0), 0.5 M Sucrose, 1 mM MgCl₂, 10 mM EDTA, 5 mM DTT, and 0.5% NP-40 (Amresco, E109), 10 mM ATP) and centrifuged at 15000 rpm for 30 min at 4°C. The supernatant was incubated with 20 µg MBP-*OssSAPK10* in a total volume of 200 µL at room temperature. The GST-*LEA12^{OR}* and GST-*LEA12⁹³⁻¹¹* were added for MBP-*OssSAPK10* stability observation.

In vitro phosphorylation assay

The in vitro phosphorylation assay was performed as previously described with slight modifications (Yu *et al.*, 2023). In brief, the purified fusion protein MBP-*OssZIP86*, GST-*OssSAPK10*, GST-*LEA12^{OR}*, GST-*LEA12⁹³⁻¹¹* and empty GST were incubated with kinase buffer including 25 mM Tris–HCl (pH 7.5), 12 mM MgCl₂, 1 mM DTT, 1 mM ATP, along with diluted total protein extracted from 93-11 at 30°C for 45 min and stopped by SDS loading buffer. Different samples of MBP-*OssZIP86* phosphorylation were detected by the Phos-tag assay with an anti-MBP antibody.

RNA in situ hybridization

The rice leaves were harvested from wild-type 93-11 seeding and immediately placed in a fixative solution (prepared with diethyl pyro-carbonate (DEPC)-treated water). RNA in situ hybridization analysis using RNA-specific probes (Table S5). After finished the hybridization process, tissue sections were observed under a Nikon microscope (Nikon Instruments Co. Ltd, Shanghai, China). Cy3 red-light excitation wavelength of 510–560 nm and emission wavelength of 590 nm. FAM green-light excitation wavelength of 465–495 nm and emission wavelength of 515–555 nm.

Statistical analyses

SPSS version 21 (IBM, Chicago, USA) was used for statistical analyses. Two tails Student's *t*-test was performed to compare two sets of data. One-way analysis of variance ($P < 0.05$) followed by Turkey's honestly significant difference (HSD) multiple comparisons tests were performed to compare multiple datasets.

Acknowledgements

National Key Research and Development Project (2022YFD1201702), The Foundation of Biological Breeding Zhongshan Lab (BM2022008-03), Scientific Innovation 2030 Project (2022ZD0401703), The Natural Science Foundation of Jiangsu Province (BK20230982, BK20220997), Jiangsu Funding Program for Excellent and Postdoctoral Talent (2023ZB492, 2022ZB351) and China Postdoctoral Science Foundation (2023 M741753) supported this study. The funding agencies had no role in the study design, data collection and analysis, decision to publish or paper preparation.

Conflict of interest

The authors declare no conflict of interest.

Author contributions

C.W. and J.W. supervised the project. Y.G., G.C. and X.C. performed the experiments. C.W. and Y.G. conceived the study

and wrote the paper. C.L., J.L., Z.D., C.Y.W. and E.D. participated in the experiments. Y.T., Y.L., Z.S., J.F.L., B.W., D.X., X.S. and H.Z. conducted and managed the fieldwork. Y.G., G.C., W.Z. and W.C. analysed data. All authors read and approved the final article.

Data availability statement

The data that supports the findings of this study are available in the supplementary material of this article.

References

- Cai, S., Chen, G., Wang, Y., Huang, Y., Marchant, D.B., Wang, Y., Yang, Q. *et al.* (2017) Evolutionary Conservation of ABA Signaling for Stomatal Closure. *Plant Physiol.* **174**, 732–747.
- Candat, A., Paszkiewicz, G., Neveu, M., Gautier, R., Logan, D.C., Avelange-Macherel, M.H. and Macherel, D. (2014) The ubiquitous distribution of late embryogenesis abundant proteins across cell compartments in Arabidopsis offers tailored protection against abiotic stress. *Plant Cell* **26**, 3148–3166.
- Chen, K., Gao, J., Sun, S., Zhang, Z., Yu, B., Li, J., Xie, C. *et al.* (2020a) BONZAI Proteins Control Global Osmotic Stress Responses in Plants. *Curr. Biol.* **30**, 4815–4825.
- Chen, K., Li, G.J., Bressan, R.A., Song, C.P., Zhu, J.K. and Zhao, Y. (2020b) Abscisic acid dynamics, signaling, and functions in plants. *J. Integr. Plant Biol.* **62**, 25–54.
- Chen, G., Xuan, W., Zhao, P., Yao, X., Peng, C., Tian, Y., Ye, J. *et al.* (2022) OSTUB1 confers salt insensitivity by interacting with Kinesin13A to stabilize microtubules and ion transporters in rice. *New Phytol.* **235**, 1836–1852.
- Deinlein, U., Stephan, A.B., Horie, T., Luo, W., Xu, G. and Schroeder, J.I. (2014) Plant salt-tolerance mechanisms. *Trends Plant Sci.* **19**, 371–379.
- Deng, P., Jing, W., Cao, C., Sun, M., Chi, W., Zhao, S., Dai, J. *et al.* (2022) Transcriptional repressor RST1 controls salt tolerance and grain yield in rice by regulating gene expression of asparagine synthetase. *Proc. Natl. Acad. Sci.* **119**, e2210338119.
- Fujii, H., Verslues, P.E. and Zhu, J.K. (2011) Arabidopsis decuple mutant reveals the importance of SnRK2 kinases in osmotic stress responses in vivo. *Proc. Natl. Acad. Sci.* **108**, 1717–1722.
- Ganguly, M., Datta, K., Roychoudhury, A., Gayen, D., Sengupta, D.N. and Datta, S.K. (2012) Overexpression of *Rab16A* gene in indica rice variety for generating enhanced salt tolerance. *Plant Signal. Behav.* **7**, 502–509.
- Gao, W., Li, M., Yang, S., Gao, C., Su, Y., Zeng, X., Jiao, Z. *et al.* (2022) miR2105 and the kinase OsSAPK10 co-regulate OsbZIP86 to mediate drought-induced ABA biosynthesis in rice. *Plant Physiol.* **189**, 889–905.
- Henry, R.J. (2022) Wild rice research: Advancing plant science and food security. *Mol. Plant* **15**, 563–565.
- Hernandez-Sanchez, I.E., Maruri-Lopez, I., Martinez-Martinez, C., Janis, B., Jimenez-Bremont, J.F., Covarrubias, A.A., Menze, M.A. *et al.* (2022) LEAging through literature: late embryogenesis abundant proteins coming of age-achievements and perspectives. *J. Exp. Bot.* **73**, 6525–6546.
- Li, X., Feng, H., Wen, J., Dong, J. and Wang, T. (2018) MtCAS31 Aids Symbiotic Nitrogen Fixation by Protecting the Leghemoglobin MtLb120-1 Under Drought Stress in *Medicago truncatula*. *Front. Plant Sci.* **9**, 633.
- Li, X., Liu, Q., Feng, H., Deng, J., Zhang, R., Wen, J., Dong, J. *et al.* (2020) Dehydrin MtCAS31 promotes autophagic degradation under drought stress. *Autophagy* **16**, 862–877.
- Li, X., Yu, B., Wu, Q., Min, Q., Zeng, R., Xie, Z. and Huang, J. (2021) OsMADS23 phosphorylated by SAPK9 confers drought and salt tolerance by regulating ABA biosynthesis in rice. *PLoS Genet.* **17**, e1009699.
- Liang, Y., Kang, K., Gan, L., Ning, S., Xiong, J., Song, S., Xi, L. *et al.* (2019) Drought-responsive genes, late embryogenesis abundant group3 (LEA3) and vicinal oxygen chelate, function in lipid accumulation in Brassica napus and Arabidopsis mainly via enhancing photosynthetic efficiency and reducing ROS. *Plant Biotechnol. J.* **17**, 2123–2142.
- Liu, C., Mao, B., Yuan, D., Chu, C. and Duan, M. (2022) Salt tolerance in rice: Physiological responses and molecular mechanisms. *Crop J.* **10**, 13–25.
- Ma, Y., Szostkiewicz, I., Korte, A., Moes, D., Yang, Y., Christmann, A. and Grill, E. (2009) Regulators of PP2C phosphatase activity function as abscisic acid sensors. *Science* **324**, 1064–1068.
- Ren, Z.H., Gao, J.P., Li, L.G., Cai, X.L., Huang, W., Chao, D.Y., Zhu, M.Z. *et al.* (2005) A rice quantitative trait locus for salt tolerance encodes a sodium transporter. *Nat. Genet.* **37**, 1141–1146.
- Sah, S.K., Reddy, K.R. and Li, J. (2016) Abscisic Acid and Abiotic Stress Tolerance in Crop Plants. *Front. Plant Sci.* **7**, 571.
- Tang, W., Ye, J., Yao, X., Zhao, P., Xuan, W., Tian, Y., Zhang, Y. *et al.* (2019) Genome-wide associated study identifies NAC42-activated nitrate transporter conferring high nitrogen use efficiency in rice. *Nat. Commun.* **10**, 5279.
- Wang, F., Zhu, D., Huang, X., Li, S., Gong, Y., Yao, Q., Fu, X. *et al.* (2009) Biochemical insights on degradation of Arabidopsis DELLA proteins gained from a cell-free assay system. *Plant Cell* **21**, 2378–2390.
- Wang, Y., Wang, C., Zheng, M., Lyu, J., Xu, Y., Li, X., Niu, M. *et al.* (2016) WHITE PANICLE1, a Val-tRNA Synthetase Regulating Chloroplast Ribosome Biogenesis in Rice, Is Essential for Early Chloroplast Development. *Plant Physiol.* **170**, 2110–2123.
- Wang, W., Mauleon, R., Hu, Z., Chebotarov, D., Tai, S., Wu, Z., Li, M. *et al.* (2018) Genomic variation in 3,010 diverse accessions of Asian cultivated rice. *Nature* **557**, 43–49.
- Wang, J., Nan, N., Li, N., Liu, Y., Wang, T.J., Hwang, I., Liu, B. *et al.* (2020a) A DNA Methylation Reader-Chaperone Regulator-Transcription Factor Complex Activates OsHKT1;5 Expression during Salinity Stress. *Plant Cell* **32**, 3535–3558.
- Wang, Y., Hou, Y., Qiu, J., Wang, H., Wang, S., Tang, L., Tong, X. *et al.* (2020b) Abscisic acid promotes jasmonic acid biosynthesis via a 'SAPK10-bZIP72-AOC' pathway to synergistically inhibit seed germination in rice (*Oryza sativa*). *New Phytol.* **228**, 1336–1353.
- Wang, J., Ren, Y., Liu, X., Luo, S., Zhang, X., Liu, X., Lin, Q. *et al.* (2021) Transcriptional activation and phosphorylation of OsCNGC9 confer enhanced chilling tolerance in rice. *Mol. Plant* **14**, 315–329.
- Welsch, R., Wüst, F., Bär, C., Al-Babili, S. and Beyer, P. (2008) A third phytoene synthase is devoted to abiotic stress-induced abscisic acid formation in rice and defines functional diversification of phytoene synthase genes. *Plant Physiol.* **147**, 367–380.
- Xie, C., Zhang, R., Qu, Y., Miao, Z., Zhang, Y., Shen, X., Wang, T. *et al.* (2012) Overexpression of MtCAS31 enhances drought tolerance in transgenic Arabidopsis by reducing stomatal density. *New Phytol.* **195**, 124–135.
- Yoshida, T., Christmann, A., Yamaguchi-Shinozaki, K., Grill, E. and Fernie, A.R. (2019) Revisiting the Basal Role of ABA – Roles Outside of Stress. *Trends Plant Sci.* **24**, 625–635.
- Yu, J., Zhu, C., Xuan, W., An, H., Tian, Y., Wang, B., Chi, W. *et al.* (2023) Genome-wide association studies identify OsWRKY53 as a key regulator of salt tolerance in rice. *Nat. Commun.* **14**, 3550.
- Zelm, E.V., Zhang, Y. and Testerink, C. (2020) Salt Tolerance Mechanisms of Plants. *Annu. Rev. Plant Biol.* **71**, 403–433.
- Zhao, C., Zhang, H., Song, C., Zhu, J.K. and Shabala, S. (2020) Mechanisms of Plant Responses and Adaptation to Soil Salinity. *Innovations* **1**, 100017.

Supporting information

Additional supporting information may be found online in the Supporting Information section at the end of the article.

Figure S1 Phenotypes of rice varieties under salt treatments at different NaCl concentrations.

Figure S2 Phenotypes of *Oryza rufipogon* Griff. and 93-11 under salt stress.

Figure S3 Phenotypic statistics of CSSLs under salt stress.

Figure S4 *LEA12* knock out plants reduced salt resistance.

Figure S5 *LEA12^{OR}* complements the salt-sensitive phenotype of *LEA12* mutant.

Figure S6 Comparison of promoters of *LEA12⁹³⁻¹¹* and *LEA12^{OR}*.

Figure S7 Comparison of CDSs of *LEA12⁹³⁻¹¹* and *LEA12^{OR}*.

Figure S8 *LEA12^{OR}* participates in osmotic adjustment under salt stress.

Figure S9 Relative expressions of salt tolerance-related genes.

Figure S10 Shoot ion contents of 93-11 and NIL-*LEA12^{OR}* under salt stress.

Figure S11 *LEA12^{OR}* confers drought tolerance in rice.

Figure S12 The expression patterns of *LEA12* and *OsSAPK10*.

Figure S13 Protein levels in the LCI assay.

Figure S14 In vitro phosphorylation assay of OsbZIP86.

Figure S15 Relative expression level of *OsNCED3*.

Figure S16 Selection and haplotype evolution of *LEA12*.

Figure S17 *LEA12^{OR}* improves ST and yield under salt stress in rice.

Figure S18 Homologous gene of *LEA12* in maize positively regulates ST.

Table S1 Eight ST-related QTLs.

Table S2 Four *ORFs* located in the LD on Chr5.

Table S3 SNP annotation of the four *ORFs* on Chr5.

Table S4 Yeast clones of the two-hybrid library screening.

Table S5 Primers used in this work.